Jurnal Teknologi, 44(F) Jun 2006: 1–12

EFFECT OF TEMPERATURE ON THE ELECTROROTATION BEHAVIOR OF HUMAN RED BLOOD CELLS

JUTIPORN SUDSIRI[1]*, DERK WACHNER[2], MARGARITA SIMEONOVA[3], JUTTA DONATH[4] & JAN GIMSA[5]

Abstract. The dielectric parameters of Human Red Blood Cells (HRBCs) were investigated by Electrorotation (ER). Suspended HRBCs were exposed to rotating electric fields in the range from 50 kHz to 250 MHz in a rectangular 4-electrode microchip chamber. ER spectra was recorded at external conductivities ranging from 0.02 – 3.00 S/m. The electrode structures were fabricated on glass chips by laser ablation of a platinum layer. Different measuring temperatures were used. At low conductivities, the temperature of the microscopic stage was kept constant by a thermostat. At higher medium conductivities, the additional temperature increase in the measuring volume due to Joule heating was registered. Measured data in the range from 20 to 35°C were then sorted according to different temperature classes of a width of 5 K. The first and the second characteristic peak frequencies of ER were plotted over medium conductivity and interpreted using an oblate single shell model with a dispersive cytoplasm and temperature dependent electric cell parameters.

Keywords: Erythrocyte, AC-electrokinetics, impedance, dispersion, ellipsoidal cell model, electric cell properties

1.0 INTRODUCTION

Electrorotation (ER) allows for investigating the dielectric properties of single biological cells without irreversible damage. For measurements, cells are suspended in electrolyte medium at a high dilution and exposed to a rotating electric field. The field induces a complex dipole moment in the cell, i.e. a moment having a real (in phase to the external field) and an imaginary (out of phase to the external field) part. For a given field frequency, the moment depends on the relative polarizability of cell and medium. The interaction of the out of phase part of the induced dipole moment and the external field leads to a torque which can be observed microscopically as the rotation of the single cells. Theoretically, the torque is given by the cross product of the imaginary part of the induced dipole moment and the external field. If the properties of the

[1,2,3,4&5] University of Rostock, Department of Biology - Chair of Biophysics, Gertrudenstr. 11A D-18057 Rostock, Germany

* Corresponding author: Tel: +49-381-494 2037, Fax: +49-381-494 2039, Email: jan.gimsa@biologie.uni-rostock.de

On leave from Prince of Songkla University, Department of Science and Technology, Suratthani Campus, Muang, Suratthani 84100, Thailand

external medium and the cell geometry are known, the electric properties of the cell and its compartments, i.e. conductivities (σ) and permittivities (ε) can be inferred from the frequency dependence of the cell rotation speed and direction [1 - 3]. At low frequencies, membrane polarization is the major component of the cell dipole moment. With increasing frequency, when the membrane polarization cannot completely follow the external field, the cell dipole moment is partly out of phase with the external field. Over a logarithmic frequency scale, the frequency dependence of the magnitude of the out of phase part of the dipole moment forms a peak, which can be detected in the electrorotation speed. Typically, peaks are of a Lorentzian shape with a characteristic half-width of one frequency decade. Naturally, the peak (charactersitic frequency f_{c1}, peak height R_1, see [4]) generated by the dispersion of the membrane polarization is mainly determined by the membrane dielectric properties. At higher frequencies, where the membrane is electrically transparent, the cellular polarization mainly arises from the difference in cytoplasmic and external medium properties. Another ER peak is observed that is caused by the transition of the polarization balance of the external and cytoplasmic media. Whereas this balance is determined by the medium conductivities at lower frequencies it is determined by their permittivities at frequencies above the conductivity dispersion. Accordingly, the second, high frequency peak of ER (charactersitic frequency f_{c2}, peak height R_2) yields information on the dielectric properties of the cytoplasm.

The development of ER microelectrode chambers allowed us to use lower driving voltages and access the dielectric parameters of biological cells at physiological [3, 5] and even higher ionic strengths of the external medium [6]. Nevertheless, problems due to Joule's heating cannot be completely avoided at high medium conductivities. Heat production is linearly related to the electric conductivity and the square of the applied voltage. A temperature increase by ΔT affects the viscosity of the external medium (η), the permittivities (ε) and the conductivities (σ) of the system in the following way:

$$\eta = \eta_{T_o} e^{-a\Delta T}, \qquad \varepsilon = \varepsilon_{T_o}(1 - b\Delta T), \qquad \sigma = \sigma_{T_o}(1 + c\Delta T) \tag{1}$$

For η_{T_o}, ε_{T_o}, and σ_{T_o}, see Table 1 and text. The temperature coefficients, a and c were assumed to be 0.02 K^{-1} for all media ([7], see also [5] and references cited therein). For the external and internal media, b has been extrapolated to 0.0046 K^{-1} from the temperature dependence of the water permittivity [7]. No temperature dependence has been assumed for the membrane capacitance (compared to the very low temperature coefficients for the permittivities of fatty acid-chain-like compounds given in [7]). The temperature dependence of the parameters leads to the alteration in the electric cell properties given in Table 1.

In our previous paper [6], we explained the deviation of the theoretical curve from the measuring points by the temperature increase in the chamber. In this paper, we

will estimate this effect by comparing ER spectra of HRBCs at different temperatures. To this end, cells were suspended at external conductivities ranging from 0.02 up to 3.00 S/m. The observation temperatures were varied in the interval from 20 to 35°C. With increasing temperature, an increase in the ER speed and a shift of the characteristic frequencies (f_{c1}, f_{c2}) toward higher frequencies has been observed. Qualitatively, the observed changes of the ER spectrum can be explained by our single shell model [4] when all parameters in the system temperature dependencies according to Equation (1) are assumed.

2.0 THEORY

For a spherical cell of radius R, the rotation speed is determined by the equilibrium of hydrodynamic friction, F_{rot} and ER torque, T. Stoke's friction law for a sphere rotating at ω_c under laminar flow conditions is given by:

$$F_{rot} = 8\pi\eta R^3\omega_c \tag{2}$$

and the ER torque acting on a spherical cell is:

$$T = \frac{4\pi R^3}{3}\varepsilon_0\varepsilon_e E^2\ \mathrm{Im}(K^*) \tag{3}$$

For $F_{rot} = T$, the rotation speed ω_c of the cell is:

$$\omega_c = \frac{T}{8\pi\eta R^3} = \frac{\varepsilon_0\varepsilon_e\ \mathrm{Im}(K^*)E^2}{6\eta} \tag{4}$$

E, ε_0, and ε_e are the electric field strength, the permittivity of vacuum and the relative permittivity of the external medium, respectively. The complex Clausius-Mossotti factor K^* is marked by an asterisk.

Please note that our electric red blood cell model is an oblate spheroid with the three semiaxes $a = b$ and c. The friction law for this shape is different from Equation (2). Nevertheless, in practice, the problem is even more complex. HRBCs are biconcave and rotate around their short axis in the vicinity of the surface of the electrode chip. For the sake of simplicity, we will therefore, not consider the absolute but only relative changes in the rotation speed.

The Clausius-Mossotti factor is the frequency dependent part of the induced dipole moment [4, 6]. For a spheroidal cell with a membrane much thinner than its semiaxes in the direction of semiaxis a, it is given by:

$$K_a^* = \frac{a_{\mathrm{inf}}}{a_{\mathrm{inf}} - a}\left(1 - \frac{Z_a^i + Z_a^m}{Z_a^i + Z_a^m + Z_a^e}\frac{a_{\mathrm{inf}}}{a}\right) \tag{5}$$

where the impedance components for cytoplasm, membrane and external medium (indices i, m and e) are given by: $Z_a^i = a/\sigma_i + j\omega\varepsilon_i\varepsilon_0$, $Z_a^m = d/\sigma_m + j\omega\varepsilon_m\varepsilon_0$, $Z_a^i = a_{\inf} - a/\sigma_e + j\omega\varepsilon_e\varepsilon_e$, respectively. a, $a_{\inf}$ and d stand for the semiaxis length, the influential radius [4] in the direction of a, and the membrane thickness, respectively. In the following, membrane conductance and membrane capacitance were calculated assuming a membrane thickness of 8 nm.

For the human red cell, we assumed the oblate cell model given in [3], with a long semiaxis of a = 3.3 µm. For an axis ratio of 1:2, an influential radius $a_{\inf}$ = 4.0 µm is obtained [4]. At 23°C the relative external permittivity, membrane conductance, and membrane capacitance were assumed to be 78.5, 125 S/m^2, and 9.97 mF/m^2, respectively [3]. For the conductivity and the relative permittivity of the cytoplasm at 23°C, frequency values of 0.4 S/m and 212 respectively, have been published [3]. The cytoplasmic permittivity disperses around 15 MHz leading to a relative permittivity of 50 and a conductivity of 0.535 S/m at high frequencies (compare to parameters in [3]). The parameters in Table 1 have been determined starting from these values.

3.0 MATERIALS AND METHODS

Two solutions, a 300 mOsM sucrose solution and a 300 mOsM NaCl solution, both containing 1 mM phosphate buffer (pH 6) were appropriately mixed to adjust the medium conductivity in the range of 0.02 to 3.00 S/m. For each experiment, 15 ml of solution was thermostated to the desired temperature prior to the suspension of 15 µl of fresh blood. 5 µl of this suspension was transferred to the measuring chamber that was pre-warmed to the observation temperature.

The chamber consisted of a rectangular 4-electrode microchip. The chip electrodes were fabricated by Laser ablation from a glass chips originally covered by a homogeneous layer of platinum of 500 nm thickness. The distance of two opposing electrode tips was about 300 µm [6]. A rotating electric fields in the range from 50 kHz to 250 MHz was produced by a radio frequency generator HP 8131A (Hewlett Packard, USA), by application of four progressively 90°-phase shifted signals of a peak-to-peak voltage of 5 V. At every conductivity, ER spectra of 5 different cells were recorded via a video system. At conductivities of 2 S/m above 25°C and at 3 S/m, no complete spectra could be recorded on single cells due to medium convections. Therefore, new cell suspension was transferred to the chamber for every measuring point. All measurements were finished within 5 minutes after cell suspension.

At the end of each experiment, the temperature of the chamber was controlled by a small thermistor. The conductivity of the suspension was measured in the temperature compensation mode (20°C) of the conductometer. To avoid cell damage by the temperature increase during the measurements, care was taken to avoid temperatures above 42°C. The obtained spectra were then fitted by a function consisting of two Lorentzian peaks, corresponding to the two major ER peaks [2].

4.0 RESULTS

Figure 1 shows ER spectra for eight selected external conductivities ranging from 0.02 – 3.00 S/m. At each conductivity, spectra for four different temperature classes are given. At low and medium conductivities (0.02 – 0.50 S/m), co- and anti-field rotation peaks are clearly visible at all observation temperatures. Starting at a conductivity of 1.00 S/m, the second peak changed its sign and only two negative peaks are observed. The temperature change did not alter the overall ER spectra shape. However, the characteristic parameters of the spectra f_{c1}, f_{c2}, R_1 and R_2 did shift (see also Figures 2 and 3). Both frequencies and the rotation speed at the peaks increased. At higher conductivities, the largest change in the parameters was observed for the temperature change from 20 to 35°C.

The dotted line represent frequency dependent parameters according to Table 1. The measuring points in Figure 2 present new data together with those already published. To calculate the theoretical curves, we assumed the cell model described above. Parameters at different temperatures are given in Table 1 (see discussion). We also checked the temperature dependence of the viscosity of our measuring solutions.

5.0 DISCUSSION AND CONCLUSION

Even though temperature dependencies of the HRBC properties have already been investigated [8 - 10], a systematic evaluation by ER has never been attempted. For impedance measurements on HRBCs embedded in the pores of a microfilter, Bao *et al.* [9] described an increase in the specific membrane capacitance from about 1 μF/cm^2 at 23°C to about 7 μF/cm^2 at 40°C. The authors explained their findings by speculative assumptions on changes in the membrane structure, like the incorporation of large amounts of water. We think that ER is an elegant method to check the temperature dependence of the membrane properties on the single cell level. Nevertheless, most authors conducted ER experiments at a constant room temperature, e.g. at about 23°C [1, 2, 7, 11]. Recently, it has been reported that temperature changes within the physiological range do shift the characteristic points of the ER spectra (f_{c1}, f_{c2}, R_1, R_2), even though the overall shape of the spectrum was not altered significantly [12].

Table 1 presents the temperature dependent parameters that we derived to obtain the theoretical curves in Figures 2 and 3. The 20°C values for the medium viscosity were extrapolated to the sucrose and salt concentrations of our measuring solutions from data given in [7]. The value for the 0.5 S/m solution was measured by a viscosimeter. Equation (1) was applied to obtain the values for the higher temperatures. The cell parameters have been extrapolated from data previously published for 23°C [3]. The cell model is featured by a cytoplasmic conductivity of 0.4 S/m and a relative permittivity of 212 at low frequencies, dispersing at 15 MHz to become 0.535 S/m and 50 at high frequencies. The table combines these data with data from

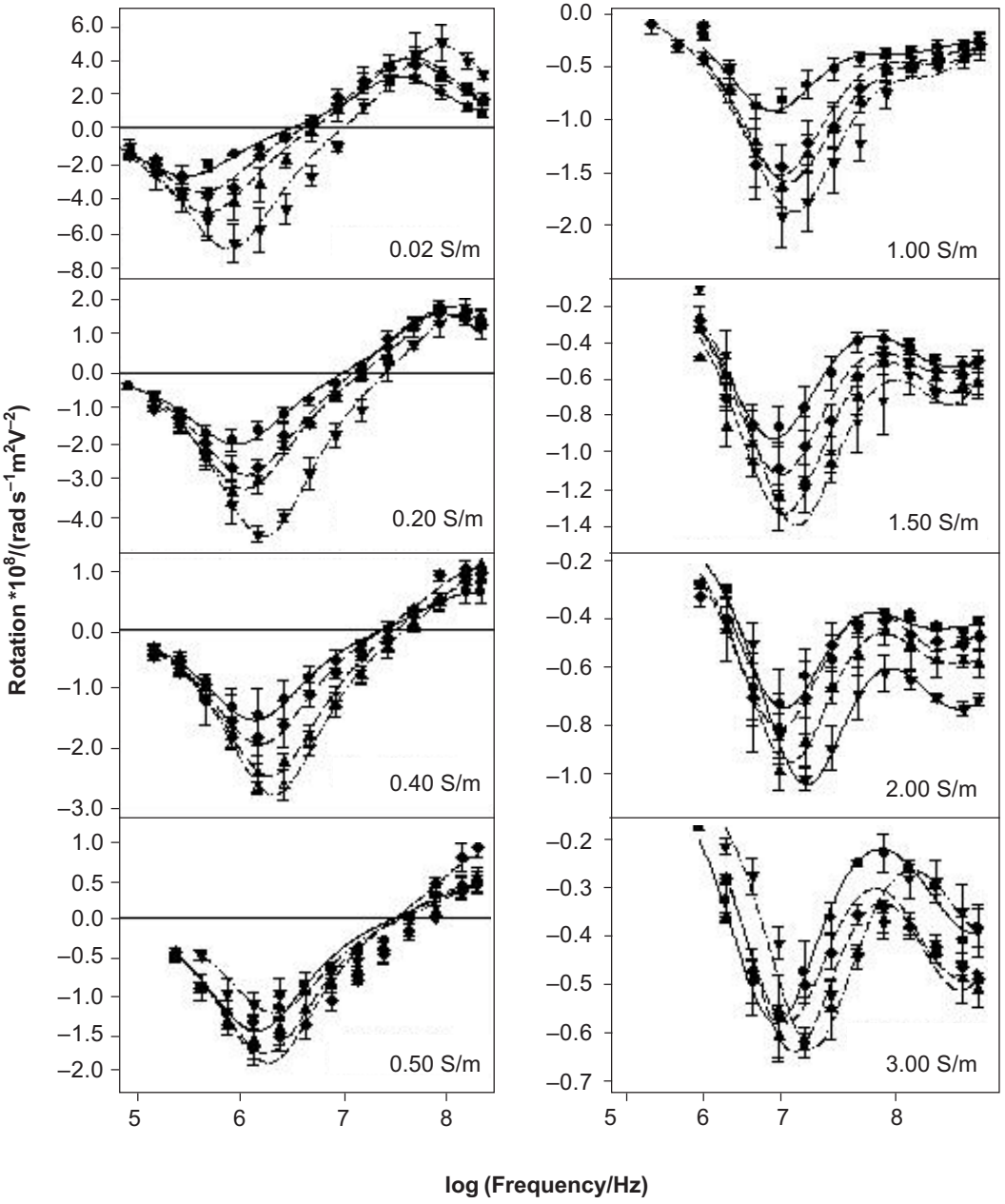

Figure 1 ER spectra at different external conductivities and for four different temperature classes, 20°C (circles), 25°C (diamond), 30°C (triangles up), and 35°C (triangles down). Each measuring point represents measurements on at least 5 cells. The conductivities given in the figures refer to 20°C value. Two superimposed Lorentzian peaks of the form $2*R*f*f_c/(f^2+f_c^2)$ have been fitted to the measuring points. R, f and f_c stand for peak rotation, field frequency, and characteristic frequency, respectively

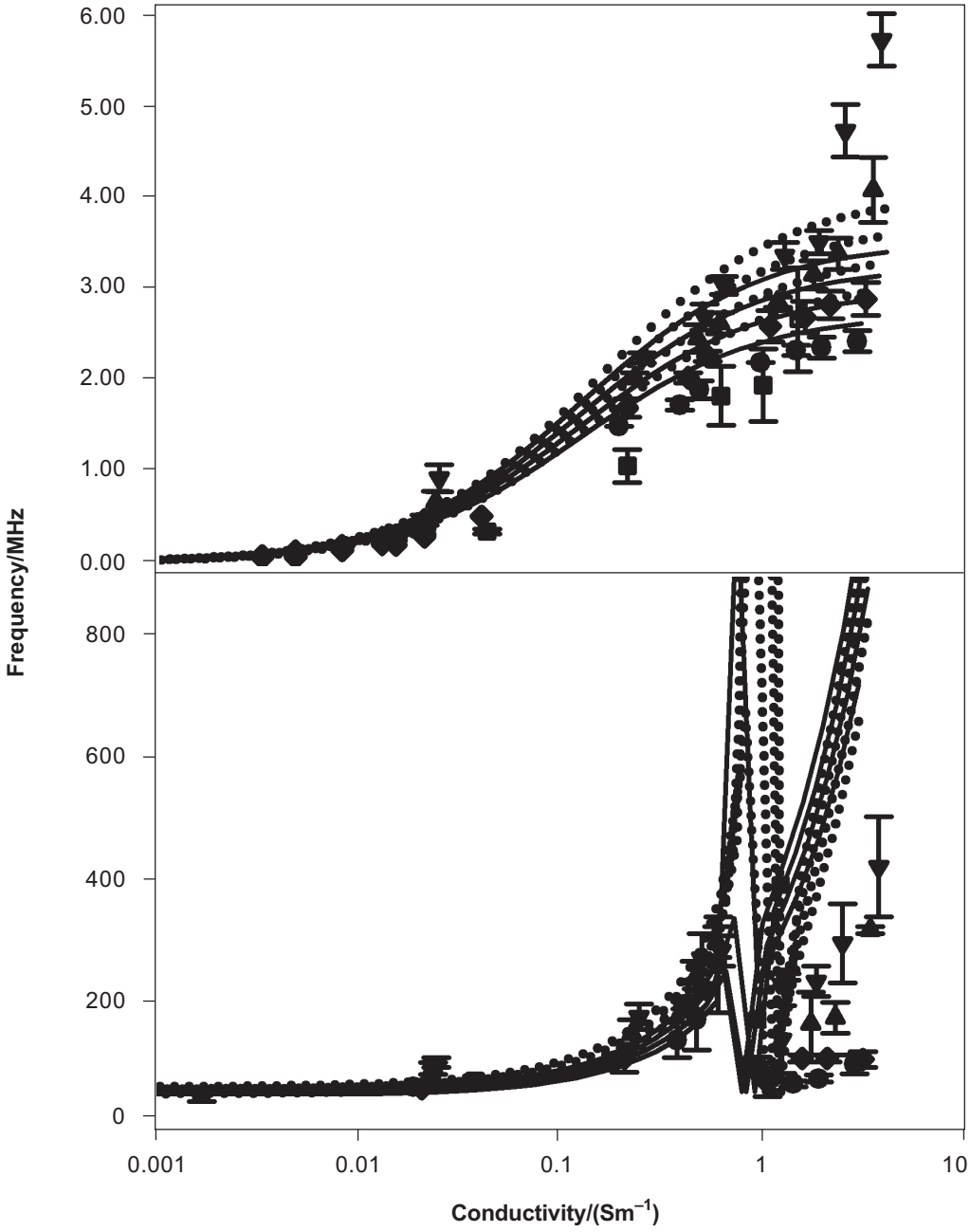

Figure 2 Fitted characteristic frequencies of Figure 1 over external conductivity and for different temperatures (for symbols see Figure 1). A and B represent the first (f_{c1}) and second (f_{c2}) characteristic frequency. Conductivities at higher temperatures were calculated from 20°C and Equation (1). Filled rhombi and filled squares represent data for 23°C already published in [11] and [3], respectively. For curves, see text

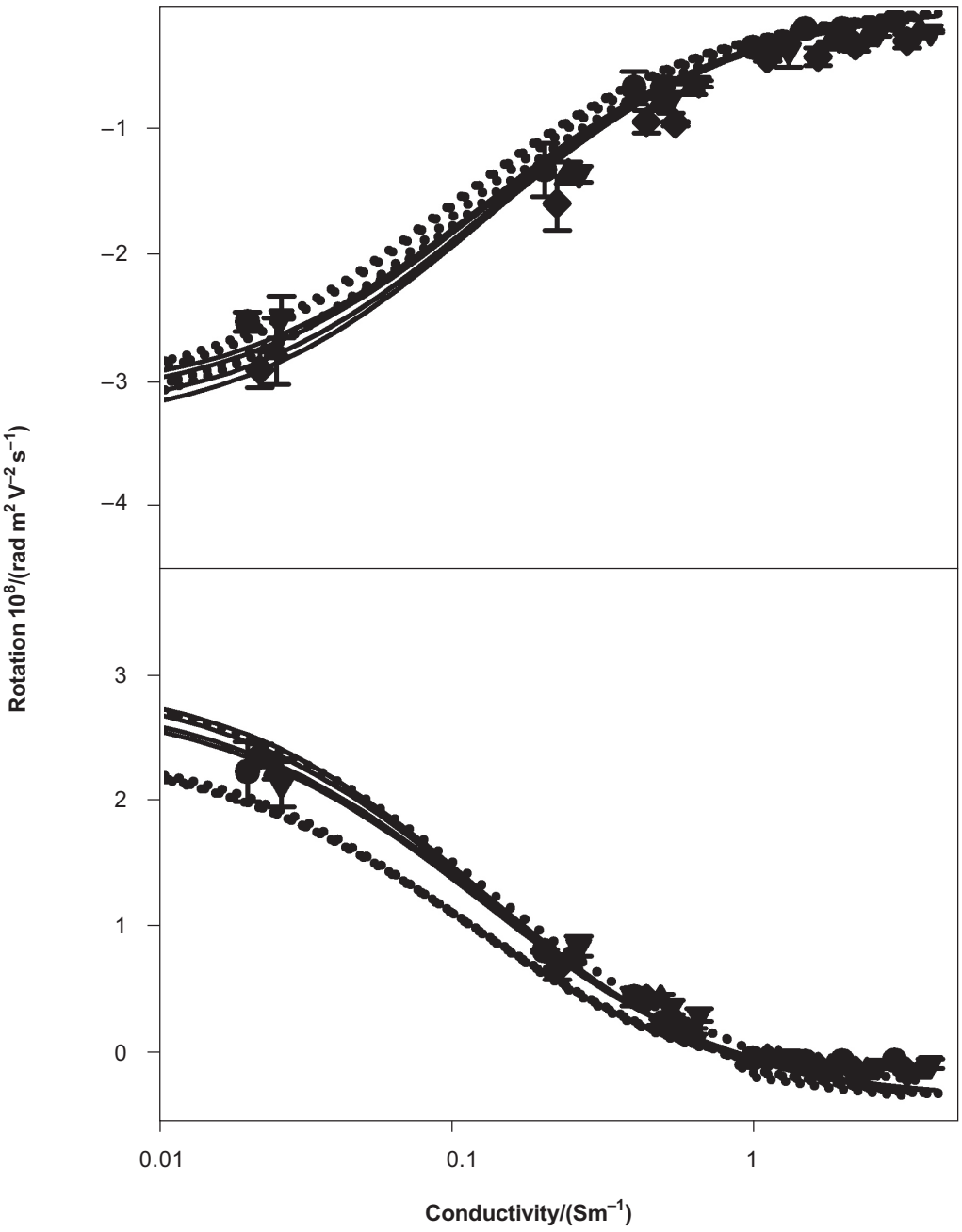

Figure 3 Rotation peak amplitudes of the first (A) and second (B) peak obtained from the spectra fits of Figure 1

the literature and new measurements. The calculations were started from a temperature dependence of the low and high frequency permittivities at 23°C, according to Equation (1). Also the low frequency (ionic) conductivity of the cytoplasm was assumed to behave according to Equation (1). The cytoplasmic conductivity at high frequencies has been calculated from this conductivity and the dielectric decrement according to the dispersion relation:

$$\sigma_i = \sigma_i^0 + \Delta\sigma = \sigma_i^0 + \varepsilon_0 \frac{\Delta\varepsilon \left(\omega^2\tau\right)^{(1-\alpha)}}{1+\left(\omega\tau\right)^{2(1-\alpha)}} \tag{6}$$

σ_i^0 and $\Delta\sigma$ are the 20°C value of the cytoplasmic conductivity and the dielectric decrement, respectively (see Table 1).

In conclusion, ER could be demonstrated to be an elegant method for detecting the temperature dependence of the electric HRBC parameters on single cells. Our experimental data could roughly be fitted by an oblate cell model with dispersive cytoplasm properties under the assumption of linear temperature coefficients. In our first approach, a temperature independent dispersion frequency has been assumed. At temperatures above 30°C, larger deviations of the theoretical curves can be observed. Nevertheless, the tremendous increase in the membrane capacitance described by

Table 1 Assumed temperature dependencies of the viscosity of the external medium for selected conductivities and electric cell parameters according to Equations (4) and (5). Viscosities at 20°C were obtained from [7] or measured (0.5 S/m). For more details see text

Parameter	**20°C**	**25°C**	**30°C**	**35°C**
Medium viscosity (mPas)				
0.02 S/m	1.27 [7]	1.15	1.04	0.94
0.10 S/m	1.25 [7]	1.13	1.02	0.93
0.50 S/m	1.06	0.96	0.87	0.78
3.00 S/m	1.03 [7]	0.93	0.84	0.76
Relative permittivity				
External	80.2	78.5	76.6	74.8
Membrane	9.04	9.04	9.04	9.04
Internal before	214.9	210.1	205.2	200.3
and after dispersion	50.7	49.5	48.4	47.2
Dielectric decrement	164.2	160.6	156.8	153.1
Conductivity (S/m)				
External	0.020 – 3.000	0.022 – 3.400	0.024 – 3.600	0.026 – 3.900
Membrane	$0.94*10^{-6}$	$1.04*10^{-6}$	$1.12*10^{-6}$	$1.24*10^{-6}$
Internal before	0.376	0.416	0.456	0.496
and after dispersion	0.514	0.551	0.588	0.624

Table 2 Correction factors for the cell rotation speed according to Equation (1) relative to sucrose solution of 0.02 S/m at 20°C. Correction factors for solutions of intermediate conductivities were linearly extrapolated. Correcting the peak rotation speeds obtained from the spectra in Figure 1 allowed us to compare rotation peak data at the same friction condition. To fit theoretical Im (K^*) curves, they were multiplied by a general friction coefficient. Figure 3 presents the corrected rotation speed

Medium viscosity (mPas)	20°C	25°C	30°C	35°C
0.02 S/m	1.00	1.10	1.22	1.35
0.1 S/m	1.02	1.23	1.24	1.34
0.5 S/m	1.20	1.32	1.45	1.63
3.0 S/m	1.23	1.36	1.51	1.67

Bao *et al*. [8] could not be observed. For improving our model, a better control of the temperature inside the ER chamber will be necessary. Also, better data for the temperature dependence of the cytoplasmic properties will be required. Our experiments suggest that the interpretation of ER data require special attention to temperature changes induced by Joule heating, especially when cells are suspended at high conductivities. Temperature dependent ER measurements may lead to a better understanding of temperature effects on the cytoplasmic and membrane properties of single biological cells.

ACKNOWLEDGEMENTS

J. Sudsiri and D. Wachner are grateful for a stipend of the Prince of Songkla University and a financial contribution from project number StSch 2002 0418A of the Bundesamt für Strahlenschutz to J. Gimsa, respectively. M. Simeonova acknowledges the DAAD for her stipend.

REFERENCES

[1] Arnold, W. M., and U. Zimmermann. 1998. Electrorotation: Development of a Technique for Dielectric Measurement on Individual Cells and Particles. *J. Electrostatics*. 21: 151-191.

[2] Gimsa, J., P. Marszalek, U. Loewe, and T. Y. Tsong. 1990. Dielectrophoresis and Electrorotation of Neurospora Slime and Murine Myeloma Cells. *Biophys. J.* 60: 749-760.

[3] Gimsa, J., T. Mueller, T. Schnelle, and G. Fuhr. 1996. Dielectric Spectroscopic of Single Human Erythrocytes at Physiological Ionic Strength: Dispersion of Cytoplasm. *Biophys. J.* 71: 495-506.

[4] Gimsa, J., and D. Wachner. 1999. A Polarization Model Overcoming the Geometric Restrictions of the Laplace Solution for Spherical Cells: Obtaining New Equation for Field- Induced Forces and Transmembrane Potential. *Biophys. J.* 77: 1316-1326.

[5] Mietchen, D., T. Schnelle, T. Mueller, R. Hagedorn, and G. Fuhr. 2002. Automated Dielectric Single Cell Spectroscopy-temperature Dependence of Electrorotation. *J. Phys. D: Appl. Phys*. 35: 1258-1270.

[6] Sudsiri, J., D. Wachner, J. Donath, and J. Gimsa. 2002. Can Molecular Properties of Human Red Blood Cells be Accessed by Electrorotation? *Songklanakarin J. Sci. Technol*. 24: 785-789.

[7] Lide, D. R. 1993. *CRC Handbook of Chemistry and Physics*. 74th edition. Boca Raton: CRC press.

[8] Bao, J. Z., C. C. Davis, and R. E. Schmukler. 1992. Frequency Domain Impedance Measurement of Erythocytes Constance Phase Angle Impedance Characteristics and a Phase Transition. *Biophys. J.* 61: 1427-1434.

[9] Bao, J. Z., C. C. Davis, and M. L. Swicord. 1994. Microwave Dielectric Measurements of Erythrocyte Suspensions. *Biophys. J.* 66: 2173-2180.

[10] Bielinska, I., and J. Terlecki. 1985. Temperature Dependence of the Dielectric Properties of Blood. Folia Histochem. *Cytobiol.* 23: 33-42.

[11] Gimsa, J., T. Schnelle, G. Zechel, and R. Glaser. 1994. Dielectric Spectroscopy of Human Erythrocytes: Investigations Under the Influence of Nystatin. *Biophys. J.* 66: 1244-1253.

[12] Jaeger, M. S., T. Mueller, Th. Schnelle, N. Teuscher, and A. Heilmann. 2002. Thermometry in Microfluidic Systems During Radio-Frequency Induced Heating. The Annual Meeting of the German Biophysical Society. Dresden, Germany.